On the Validation of Snow Densities Derived from SNOWPOWER Probes in a Temperate Snow Cover in Eastern Canada: First Results

M. NIANG[1], M. BERNIER[1], Y. GAUTHIER[1], G. FORTIN[1],
E. VAN BOCHOVE[2], M. STACHEDER[3], AND A. BRANDELIK[3]

ABSTRACT

In situ validation of remote sensing images of snow, monitoring greenhouse gas emissions and more accurate forecasting of water input to large hydraulic basins from snowmelt in remote areas can be supported through the development of new automatic snow measurement sensors, like the SNOWPOWER probe. This German technology consists of a flat band cable, usually 10 m long, through which high and low frequencies measurement data sets are made with a Time Domain Reflectometer (TDR) and an impedance analyser. When the cable is completely or partly embedded into the snow cover, it gives real time and continuous corresponding density and liquid water content measurements. The SNOWPOWER probe prototype is being tested in Switzerland and in Eastern Canada, at the J-C Chapais Experimental Farm (Agriculture and Agrifood Canada) near Quebec city. At this site, four flat cables were installed prior to the winter of 2002-2003. A series of weekly measurements have been conducted to monitor their behaviour in a moderate continental climate (*Dfb*) and to validate the algorithms for determining snow wetness and density. In this paper, we discuss the quality of those high and low frequency measurements. We also compare the snow parameter estimations with field data.

Key Words: SNOWPOWER, sensor, snow density, snow wetness, TDR

INTRODUCTION

Knowing the snow characteristics is essential for many applications in snow hydrology, like improvements in avalanche forecasting and prognoses of flooding events caused by melting processes. It is also mandatory for hydraulic basin and reservoir efficient management for a company such as Hydro-Québec, generating 93% of its electricity production from hydro power stations. In Canada, Clair and Ehrman (1998) showed that 41% of the annual discharge occurs in spring, as a consequence of the snow cover melting. Snow cover status and filling stage of the reservoirs have to be known for accurate optimization purposes. The snow properties also play a role in the greenhouse gas emission, as it can trap gases released from the underlying ground, particularly in agricultural areas.

The most often measured snow characteristics are the snow water equivalent (SWE), (which depends on the snow depth and density) and the snow liquid water content. Most of the time, these

[1] INRS-ETE, 2800 rue Einstein, CP 7500, Sainte-Foy (Québec), Canada, G1V 4C7
[2] Soils and Crops Research and Development Centre, Agriculture and Agri-Food Canada, 2560, boul. Hochelaga, Sainte-Foy (Québec), Canada, G1V 2J3
[3] Institut dur Meteorologie und Klimaforschung, Postfach, 3640, D-76021, Karlsruhe, Deutchland

characteristics are measured through manual snow sampling and/or estimated with hydrological models at the basin scale. The manual sampling is costly, particularly in large and remote areas, and it leads to major uncertainties (Martin et al., 1999), due to the resolution of the data, their volume and their discontinuous nature, which are not adequate to achieve representative values for natural snow covers with large spatial variability.

Therefore, a new sensor has been developed, with the capability of monitoring the snow cover over the entire winter cycle and over a larger area. This sensor system, known as SNOWPOWER probe, is especially suited for continuous measurements over long periods (Brandelik and Hübner, 1997; Huebner and Brandelik, 2000). Such a probe is presently being tested in Switzerland (alpine test site) and in Canada (agricultural test site). This paper presents the first results obtained at the Canadian test site in the winter of 2002-2003, with a focus on the determination and validation of snow density.

STUDY SITE

The research site (figure 1) is located in an open field at the J.-C. Chapais Experimental Farm of Agriculture and Agri-food Canada, near Quebec city, P.Q., Canada (46˚46'18"N, 71˚12'15"W). The field has a mostly flat surface with a slope of 0-0.5%. The site has previously been described in van Bochove et al. (2000). An automated weather station installed on the site records different meteorological parameters such as air, snow and soil temperatures, etc. (Fortin et al, 2002).

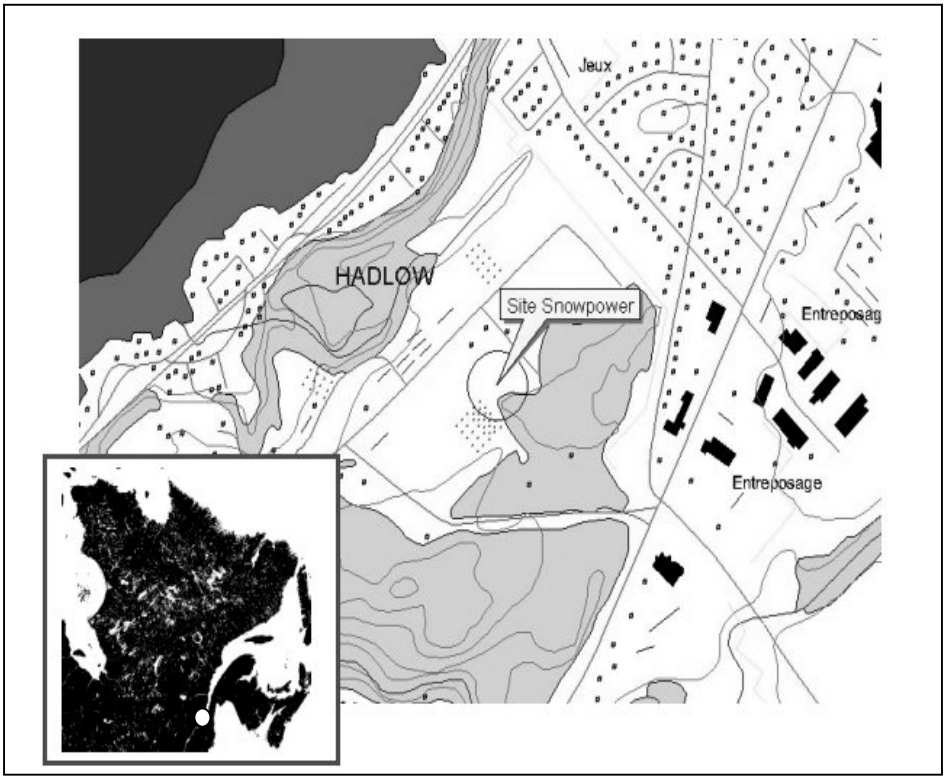

Figure 1: Study site location.

SENSOR DESIGN

The SNOWPOWER probe consists of a flat band cable (at least 10 m long), behaving like a TDR transmission line. It is installed prior to winter and therefore, it is gradually covered by snow, resulting in changes of media surrounding morphology. Through the snow season, a combination of time domain and low frequency measurements are used to determine both snow wetness and snow density. Probes have been designed with two different material thickness so far: 1,5 mm, designated as a thin cable, and 3,8 mm as a thick cable.

The probe is based on the fact that an electromagnetic wave travelling along the cable is modified by the surrounding moist material. The dielectric constant of this material ε_m, in our case, snow, can be determined in time or frequency domain, like travel time, impedance, attenuation, phase-shift, and cross talk. We measure ε_m^{hf} with a time domain reflectometer and ε_m^{lf} with an impedance analyser. With a multiplexed and cross-laid network of cables the snow moisture and density can be measured quickly and accurately over large areas.

However, around the sensor surface, an unavoidable air gap builds up due to solar radiation and the hydrophobic character of the sensor material. This gap causes underestimations of ε_m. In order to detect the air gap and enable its correction, the sensor cable consists of three conductive wires moulded within a white insulation material. The three wires can be measured in two modes, with small and with large spacing. In the case of a large spacing, the air gap has less influence on the measurement of the dielectric coefficient than in the small spacing mode. This influence can be calculated and a correction equation can be derived (Hubner and Brandelik, 2000). A software taking this problem into account was implemented by Shlaeger (2002; 2003) and is used for our simulation. This way we can determine the true ε_m without disturbing the snow cover and the air gap. Let's emphasize that results are showing, at this point, that thin cable is more sensitive than the thick one.

INSTALLATION DESIGN

The physical installation of the sensor in Canada was developed around three objectives: (1) to test different support types and to find the one most suitable for this environment; (2) to acquire data on a larger surface for inputs into hydrological models and comparison with remote sensing images and (3) to get a diversified dataset in order to better validate the measurements.

Four SNOWPOWER 10 m flat band cables have been installed at the experimental site in the fall of 2002. Two thick cables and two thin cables are being tested. To obtain data on the larger area possible, we designed a "star shaped" installation using three sloping SNOWPOWER cables (two thick and one thin) starting from a central point, 1.5 m above the ground, oriented in opposite directions at a 120º angle and ending to the ground level (Figure 2). The covered area is approximately 300 m². The other thin cable has been installed horizontally (horizontal cable), at 25 cm above the ground.

Through 32 m coaxial cables, each sensor was hooked up to a multiplexer into a heated shelter (15°C). Each cable was sequentially selected for Time Domain Reflectometer (TDR) and impedance analyzer measurements, a computer controlled process.

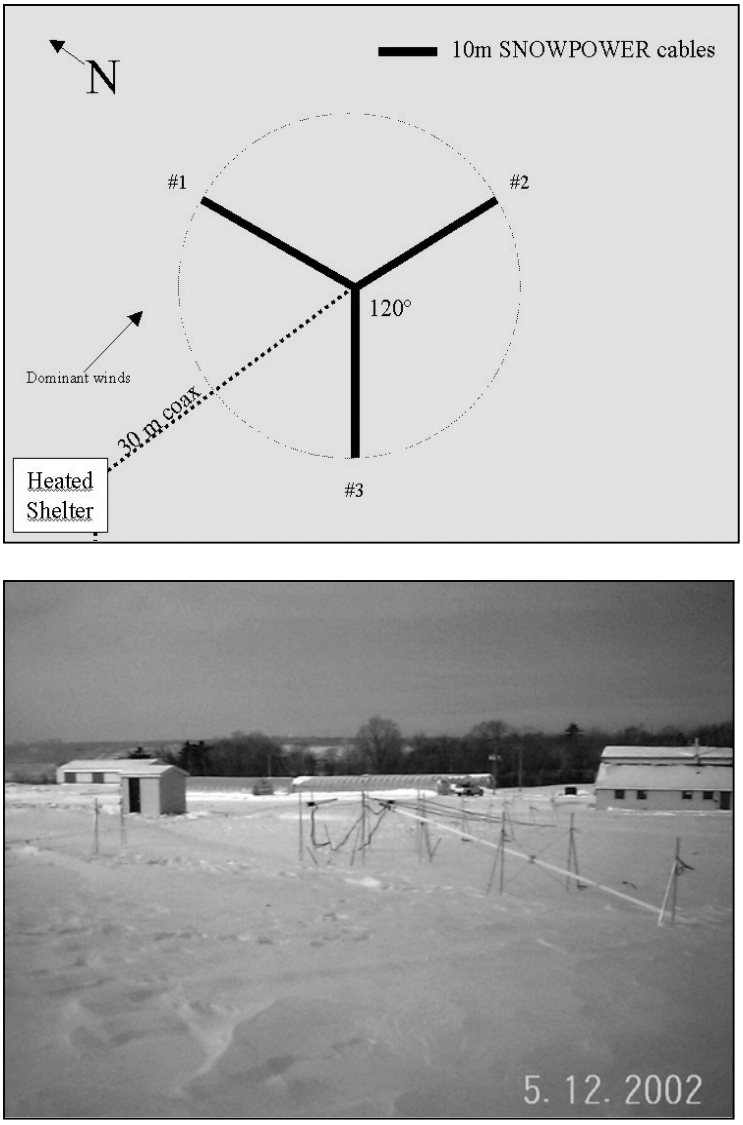

Figure 2: SNOWPOWER sensor installation at the Canadian experimental site.

SNOW MODEL

The snow pack consists of three materials (water *W*, ice *I* and air *A*). For the determination of the unknown volumetric fractions of these three materials, we need three independent equations to receive these three fractions (Brandelik et al.1999). We use one high-frequency (*hf*) measurement of the dielectric constant of snow ε_m^{hf} and one low-frequency (*lf*) measurement at a given frequency ε_m^{lf} :

$$1 = W + I + A \tag{1}$$

$$\left(\varepsilon_m^{hf}\right)^\alpha = W\left(\varepsilon_W^{hf}\right)^\alpha + I\left(\varepsilon_I^{hf}\right)^\alpha + A\left(\varepsilon_A^{hf}\right)^\alpha \tag{2}$$

$$\left(\varepsilon_m^{lf}\right)^\alpha = W\left(\varepsilon_W^{lf}\right)^\alpha + I\left(\varepsilon_I^{lf}\right)^\alpha + A\left(\varepsilon_A^{lf}\right)^\alpha \tag{3}$$

They form a linear equation system with a 3x3 matrix, which only has to be inverted for the calculation.

$$\begin{pmatrix} 1 & 1 & 1 \\ \left(\varepsilon_W^{hf}\right)^\alpha & \left(\varepsilon_I^{hf}\right)^\alpha & \left(\varepsilon_A^{hf}\right)^\alpha \\ \left(\varepsilon_W^{lf}\right)^\alpha & \left(\varepsilon_I^{lf}\right)^\alpha & \left(\varepsilon_A^{lf}\right)^\alpha \end{pmatrix} \begin{pmatrix} W \\ I \\ A \end{pmatrix} = \begin{pmatrix} 1 \\ \left(\varepsilon_m^{hf}\right)^\alpha \\ \left(\varepsilon_m^{lf}\right)^\alpha \end{pmatrix} \tag{4}$$

in which $\varepsilon_W^{hf} = \varepsilon_W^{lf} = 88$, $\varepsilon_A^{hf} = \varepsilon_A^{lf} = 1$, and $\varepsilon_I^{hf} = 3.16$ are independent from temperature and used frequency. These measurements represent the mean values of the high- and low-frequency dielectric coefficients of the material along the sensor cable. In the equations (1)-(4) instead of $\alpha = 0.5$ (Birchak et al., 1974) we use $\alpha = 0.3$ (Looyenga, 1965), which is more useful for snow mixtures. From (1), (2) and (3), one can determine the volumetric fractions W, I and A and calculate the snow density.

$$D = W\,\rho_W + I\,\rho_I \tag{5}$$

With the density of water ρ_W=0.9999 g/cm^3 and ice ρ_I=0.9150 g/cm^3 at 0°C.

Therefore one has to take into account that the different temperatures generate a change in the snow structure (melting process, ice up process), which has a much larger influence to the density than the influence of the different dielectric properties of ice under a given temperature.

Recent investigations in snow moisture determination at the Karlsruhe Research Center (Shlaeger, 2003b) showed that the temperature has a major influence on the low-frequency dielectric constant of ice (temperature range -30 to 0 °C). The dielectric constant of ice also depends on the frequency which was used for the measurements.

In order to determine the temperature dependent relaxation frequency, several low-frequency snow measurements were performed. Based on their work, the dielectric constant can be calculated by:

$$\varepsilon_I^{lf}(f,T) = \mathrm{Re}\left(\varepsilon_\infty + \frac{\varepsilon_S - \varepsilon_\infty}{1 + \sqrt{-1}\cdot f / f_{rel}(T)}\right) \text{ using } f_{rel}(T) = \frac{1}{2\pi}\cdot 10^{-\left(\frac{664.873}{T} - 7.447\right)} \tag{6}$$

in which ε_∞=3.16, ε_s=92.0205, and temperature T in Kelvin.

The dielectric constant of ice in low-frequency can be received from (6). Then the equation (3) can be substituted by :

$$\left(\varepsilon_m^{lf}(f,T)\right)^\alpha = W\left(\varepsilon_W^{lf}\right)^\alpha + I\left(\varepsilon_I^{lf}(f,T)\right)^\alpha + A\left(\varepsilon_A^{lf}\right)^\alpha \tag{7}$$

The influence of the temperature to the density of ice is very small (Lindmark, 1999) and can be neglected in our case. We always use the temperature independent density of ice ρ_{ice} = 915 kg/m^3.

The equations (1), (2) and (7) represent the solution of our problem if we use high and low frequency data. But it is also possible to use only low-frequency data, because of their frequency dependency. One has to make sure that the chosen frequencies f_1 and f_2 are not to close together. E.g. use f_1 = 6kHz *and* f_2 = 50kHz (The higher frequency takes the part of the high-frequency measurement in Eq. (2).

$$1 = W + I + A \tag{8}$$

$$\left(\varepsilon_m^{lf}(f_1,T)\right)^\alpha = W\left(\varepsilon_W^{lf}\right)^\alpha + I\left(\varepsilon_I^{lf}(f_1,T)\right)^\alpha + A\left(\varepsilon_A^{lf}\right)^\alpha \tag{9}$$

$$\left(\varepsilon_m^{lf}(f_2,T)\right)^{\alpha} = W\left(\varepsilon_W^{lf}\right)^{\alpha} + I\left(\varepsilon_I^{lf}(f_2,T)\right)^{\alpha} + A\left(\varepsilon_A^{lf}\right)^{\alpha} \quad (10)$$

Equations (1), (2) and (7) or (8)-(10) are only used for the determination of the mean values of the volume fractions of water, ice and air (and of the snow density).

DATA ACQUISITION

From December 18, 2002 to March 20, 2003, weekly SNOWPOWER measurements (high and low frequencies) were made. From March 20 to April 14 (melting season), SNOWPOWER data have been collected almost daily. Throughout the season, concurrent field data have been acquired. Every week, 12 snow cores were collected to measure snow depth (cm), Snow Water Equivalent (SWE, mm) and the mean snowpack density (kg m^{-3}) around the SNOWPOWER cables. A weekly snow profile was also done at the test site. During the melting season, at the time of the SNOWPOWER measurements, another snow profile was done near cable #3, giving the snow temperature, density and liquid water content at every 10 cm.

RESULTS AND DISCUSSION

During the 2002-2003 winter, no significant rain or melting event had happened, leaving the snow cover relatively dry from the beginning of January through mid-March (Figure 3). During that period, the diurnal air temperature stayed generally below the freezing point. On March 20, the melting period began with an increase of air temperatures steadily above zero, combined with significant rainfall events and no refreezing period until March 31. From there through April 9, the air temperature dropped back below 0ºC and the snowpack refreezed completely. After that, a cycle of diurnal melting followed.

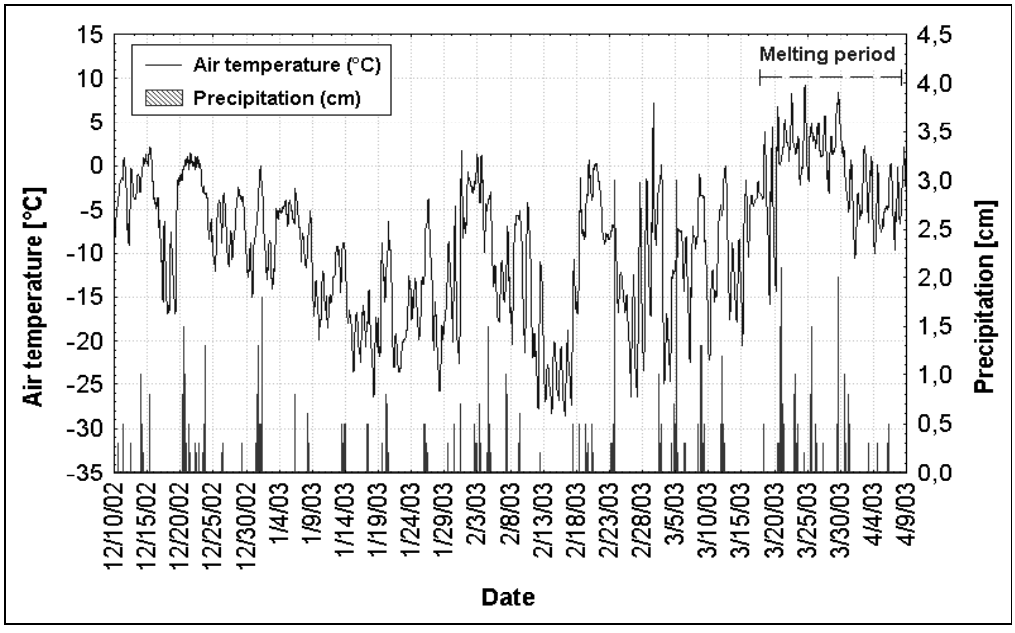

Figure 3: Daily variations of air temperature and precipitation.

Prior to March 20, the density of the snowpack had slowly increased by way of metamorphism and compaction of snow. The observed snow density had increased more rapidly during the

springmelt period, which is in accordance with other observations made for various climates in Canada (Pomeroy and Gray, 1995).

Considering the heterogeneous spatial distribution of the snow at the test site, we present in Figure 4 an averaged snow density and snow depth for the 3 snow samples near cable #3.

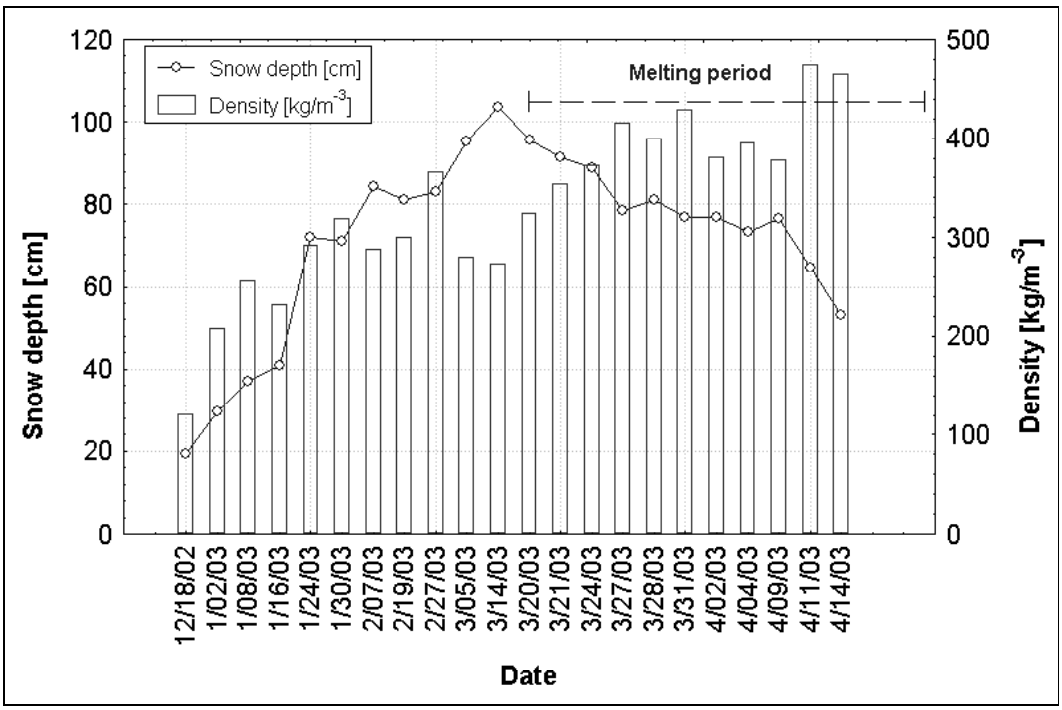

Figure 4: Reference data of the snow cover near cable #3.

This paper focuses on the results obtained during the March 20 to April 9 period (melting and refreeze), with the SNOWPOWER cable #3 (thin cable), which has been previously calibrated. Table 1 gives the mean, minimum and maximum air temperature recorded every day of measurements.

Table 1. Mean, maximum and minimum air temperature recorded every day of measurements.

Date	Air T_{mean} (°C)	Air T_{max} (°C)	Air T_{min} (°C)
3/20/03	-2,59	6,80	-14,40
3/21/03	2,63	5,30	0,50
3/24/03	3,00	9,30	-1,10
3/25/03	2,18	4,90	-1,70
3/26/03	3,25	4,90	1,60
3/27/03	2,65	5,80	0,90
3/28/03	0,88	3,40	-3,10
3/31/03	-2,93	0,60	-6,40
4/02/03	-1,53	2,30	-5,60
4/04/03	-6,01	0,10	-10,10
4/09/03	0,90	11,10	-8,70

SNOWPOWER LOW FREQUENCY MEASUREMENTS

Figure 5 shows the capacitance values measured with the impedance analyzer for several dates of the melting period. We have included the measurements of 12/18/02, which corresponds to the beginning of snow accumulation on the ground. We can clearly see two groups of capacitance, corresponding to the melting and refreezing period. Usually the spring melting period starts gently with a diurnal-nocturnal thaw-refreeze period, followed by a more intensive melting period (isothermal snowpack state). As we described earlier, the 2002-2003 winter started with an intensive melting period, followed by a thaw-refreeze period.

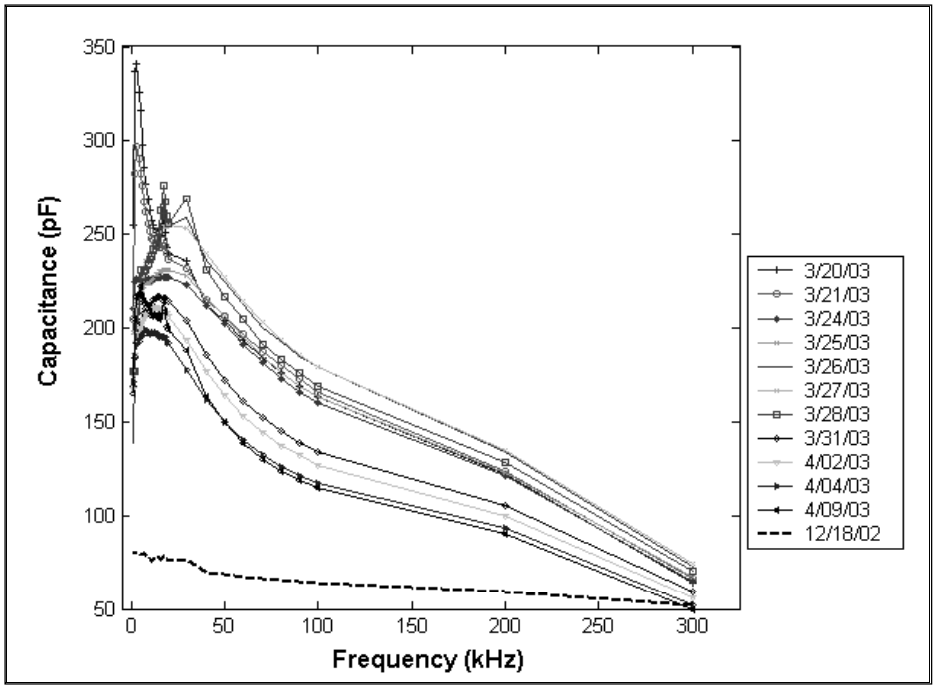

Figure 5 : Capacitances values for the dates under study

Zooming on the 50 to 100 kHz frequencies (Figure 6) we can see more specifically, three groups of data. They correspond to these environmental conditions:

- Melting period: From March 20 to March 25, the air temperature was steadily above 0ºC. A heavy rainfall event happened from late March 20 to the next morning. Despite all this incoming water, the wet front advance was limited to the top layers because of the low temperatures in the snowpack. As mentioned by Marsh and Woo (1984) when the water percolates from the surface to the underlying and below zero snow layers, the water front advance tends to create both ice fingers and horizontal ice layer. So the underlying layers stayed relatively cold and dry on March 21 (Figure 7, table 1).
- Isothermal state: On March 26 and 27, the snow cover was completely in an isothermal state. Another rain event occured. All snow layers shows significant liquid water content (>3%). The capacitance values are at their highest (figure 6).
- Refreezing period : from March 31 to April 9, the air temperatures decreased below the freezing point Gradual refreezing of the entire snow cover (Figure 7). Intense snow compaction. Significant drop of the capacitance values (Figure 6).

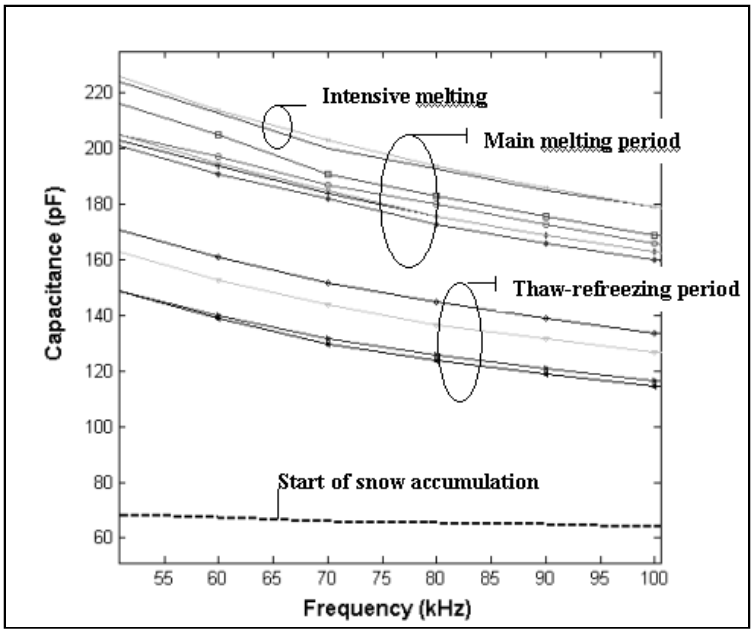

Figure 6: Zoom on the 50 to 100 kHz frequencies

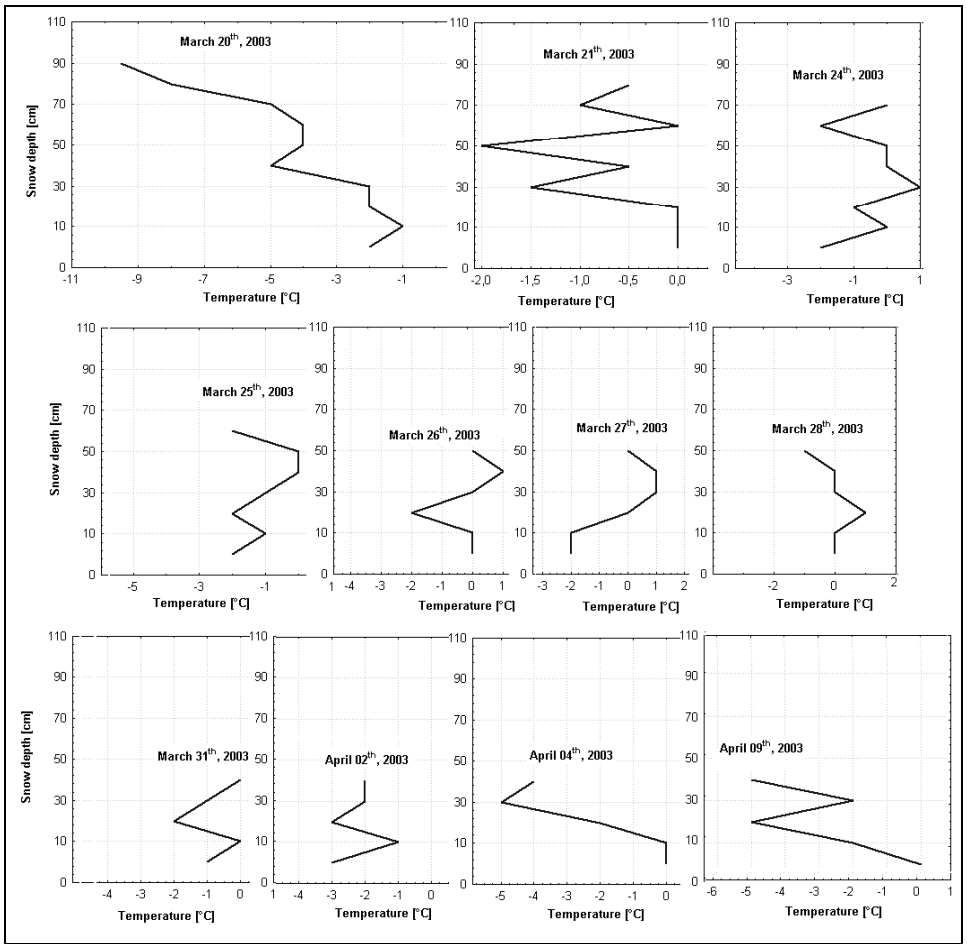

Figure 7: Temperature profiles for dates under study

These data confirm the sensitivity of the probe to snow properties changing. The capacitance values depend on the dielectric constant of the surrounding medium. At low frequency there is an influence of snow crystal shape on the dielectric constant (Hubner and Brandelik, 2000) which is a function of temperature, as expressed by equation (6).

SNOWPOWER HIGH FREQUENCY MEASUREMENTS

The high frequency measurements also show a sensitivity to the snow properties. Figure 8a shows the difference of the wave travel time along the cable and the transition zones between air and snow for selected dates corresponding to the melting period. We can notice the difference of the reflection of the TDR signal at the beginning and the end of the sensor cable and the values of the transition point (Traveltime) air - snow. It is well-known that at high frequency there is no temperature and frequency dependence on the dielectric constant (Tirui et al. 1984). Therefore the dielectric constant is mainly a function of snow density and wetness.

From March 20 to 25 (Figure 8b), warmer air temperatures and rainfalls caused a decrease of the temperature gradient within the snow cover and snow melt. Liquid water content is present in the top layers and gradually moves downward. It is only on March 24 that the liquid water content started to modify the TDR trace, with a small bump that appears at the beginning of the curve.

On March 26 and 27 (Figure 8c), the remaining snow cover has reached a complete isothermal state. All snow layers show significant liquid water content (>3%), which produce significant variations of the voltage pattern at the beginning of the curves and smaller changes at the end of the curves.

From March 28 to April 9 (Figure 8d), temperature drops back below the freezing point. The snow liquid water content gradually decreases to 0% in all layers of the remaining snow cover. The bumps at the beginning of the curves are now related to the intense compaction of the snow pack in this period.

SNOW DENSITY ANALYSIS

As explained in previous sections, the snow density was calculated using the high and low frequency measurements of the SNOWPOWER sensor (cable #3).

Figure 9 shows the comparison between these densities and the field measurements. It also shows the values of the calculated dielectric constant. The mixing rule used here is Looyenga's semiempirical dielectric formula, which provides the best results. We notice a good agreement between measured and calculated density, which are also correlated with the observed environmental conditions. The correlation coefficient is 91%. However, it should be noted that the accuracy of the validation data is dependant on the accuracy (±4%-5%) of the density measurement devices (Gauthier et al, 1997). Moreover, on April 4 and 9, the refrozen snow was too hard to manually take reliable density measurements. As for the dielectric constant, it varies accordingly with the increase and decrease of the snow liquid water content.

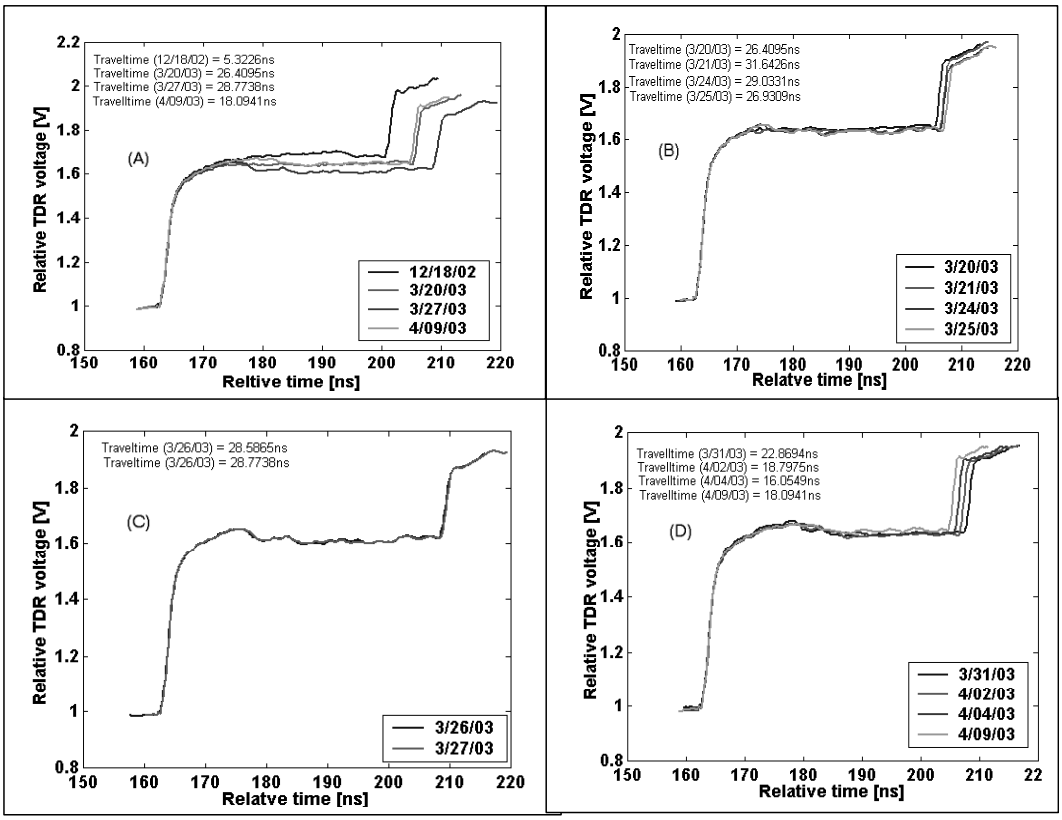

Figure 8: TDR traces for a) selected dates representing different snow cover conditions, b) melting period, c) isothermal state, d) refreezing period.

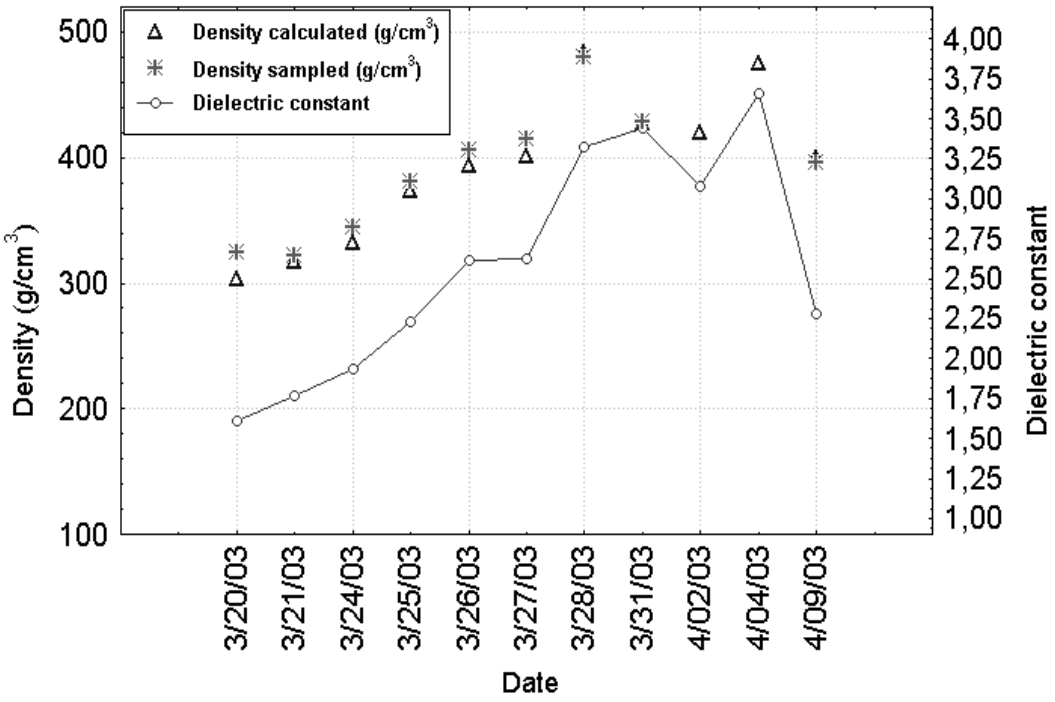

Figure 9: Validation of SNOWPOWER calculated densities.

CONCLUSION

The validation of the SNOWPOWER dataset acquired in a temperate snow cover in Eastern Canada during March through April 2003 shows very good results, concordant with the recorded meteorological data. Both high and low frequency measurements are influenced by the metamorphism of the snow properties (density, liquid water content). The comparison between the calculated snow densities using the SNOWPOWER probe and the manually measured densities shows a correlation coefficient of 0.91 and a Root Mean Square Error (RMSE) of 4%. For the melting through isothermal period, the calculated RMSE is as good as 3% and for the refreezing period, the RMSE is 5%. This increase of the RMSE is due to the difficulty to get a good sample in the hard refrozen snow. In light of these first results, the SNOWPOWER probes seem to give reliable results and represent an operational tool for continuous monitoring of the snow cover properties.

ACKNOWLEDGEMENT

The authors would like to acknowledge Stefan Schlaeger (Karlsruhe Research Center) and Luc Martel (Hydro-Québec) for their significatif contribution to this international project (SNOWPOWER) and their contract/grant sponsors: NSERC, Special Opportunity Research Programme, Ottawa, Canada, Hydro-Québec, Montréal, Canada, and the European Commission, Fifth Framework Programme, Bruxel, Belgium.

REFERENCES

Birchak JR, Gardner CG, Hipp JE, Victor JM. 1974. High dielectric constant microwave probe for sensing soil moisture. *Proceedings of IEEE*, **62** : 93-98.

Brandelik A, Huebner C. 1997. Large-area, long-term monitoring of mineral barrier materials. *Proceedings of the 1997 International Containment Technology Conference and Exhibition*, St. Petersburg, Florida, February 9-12 1997, pp. 1060-1066.

Brandelik A Huebner C, Doepke G, Wunderle S. 1998. Advanced ground truth for snow and glacier sensing. *Proceedings of the IEEE International Geoscience and Remote Sensing Symposium,* Seattle, Washington, July 6-10 1998, pp. 1873-1875.

Clair TA, Ehrman JM. 1998. Using neural networks to assess the influence of changing seasonal climates in modifying discharge, dissolved organic carbon, and nitrogen export in eastern Canada rivers. *Water Resources Reseach*, **34** : 447-455

Fortin G, Jones HG, Bernier M, Schneebeli M. 2002. Changes in the Structure and Permeability of Artificial Ice Layers Containing Fluorescent Tracer in Cold and Wet Snow Cover. *59th Eastern Snow Conference Proceedings, Stowe*, June 5-7 2002, pp. 257-266.

Gauthier, Y, Bernier M, Fortin JP, Gauthier R et Lelièvre M. (1997). Importance des mesures de terrain dans l'établissement d'algorithmes de suivi du couvert de neige à partir d'images radar. VIIe Journée Scientifique du Réseau de Télédétection de l'AUPELF-UREF, 13-17 octobre 1997, Sainte-Foy, Québec, pp. 37-43.

Hübner C, Brandelik A. 2000. Distinguished Problems in Soil and Snow Aquametry. *In Sensors Update*, Chapter 13, Baltes, H., Goepel, W. and Hess, J. (Eds.), **7**: 317-340.

Huebner C, Brandelik A, Wunderle S, Beppler D. 1997. Ground truth for soil and snow moisture sensing. *Proceedings of the 7th Internat. Symposium on Physical Measurements and Signatures in Remote Sensing*, Courchevel, France, April 7-11, **1** : 281-286.

Lindmark S. 1999. Mechanism of Salt Frost Scaling on Portland Cement-bound Materials: Studies and Hypothesis, PhD-Thesis, Lund University.

Looyenga H. 1965. Dielectric Constant of Heterogeneous Mixtures, *Physica*, **31** : 401-406.

Martin D, Bernier M., Sasseville JL et Charbonneau R. 1999. Évaluation financière de l'intégration de technologies satellitaires pour le suivi du couvert nival, au sein d'une entreprise hydroélectrique. International Journal of Remote Sensing, **20**(6) : 2033-2048.

Marsh P, Woo MK. 1984. Weeting front advance and freezing of meltwater within a snow cover. 1. Observations in the Canadian Arctic. *Water Resources Research*, **20** : 1853-1864.
Pomeroy JW, Gray DM. 1995. Snowcover; accumulation, relocation and management. National Hydrologic Research Institute Science Report no 7, Saskatoon, Saskatchewan, 144 p.
van Bochove E, Thériault G, Rochette P, Jones HG, Pomeroy JW. 2001. Thick ice layers in snow and frozen soil affecting gas emissions from agricultural soils during winter. *Journal of Geophysical Research – Atmospheres*, **106** : 23 061-23 071.
Schlaeger S. 2002. Inversion von TDR-Messungen zur Rekonstruktion räumlich verteilter bodenphysikalischer Parameter, Dissertation, Institut für Bodenmechanik und Felsmechanik, Universität Karlsruhe, Februar 2002, Veröffentlichungen des Institut für Bodenmechanik und Felsmechanik, Heft 156 (In German).
Schlaeger S. 2003. GetMoisture User manual, User-friendly *MATLAB*-Program for Soil- and Snow Moisture Evaluation (Version 1.4, 15. March 2003, translated by Dr. Markus Stacheder), 17 p.
Schlaeger S. 2003b. Personnal communication.
Tirui MT, Sihovola AH, Nyfors EG, Hallikainen MT. 1984. The Complex Dielectric Constant of Snow at Microwave Frequencies. *IEEE Journal of Oceanic Engineering*, **9**: 377-382.